DOI: 10.1534/genetics.110.114009

Hearing in Drosophila Requires TilB, a Conserved Protein Associated With Ciliary Motility

Ryan G. Kavlie,* Maurice J. Kernan† and Daniel F. Eberl*,[1]

**Interdisciplinary Graduate Program in Genetics and Department of Biology, University of Iowa, Iowa City, Iowa 52242 and †Department of Neurobiology and Behavior, State University of New York, Stony Brook, New York 11974*

Manuscript received January 10, 2010
Accepted for publication February 19, 2010

ABSTRACT

Cilia were present in the earliest eukaryotic ancestor and underlie many biological processes ranging from cell motility and propulsion of extracellular fluids to sensory physiology. We investigated the contribution of the *touch insensitive larva B* (*tilB*) gene to cilia function in *Drosophila melanogaster*. Mutants of *tilB* exhibit dysfunction in sperm flagella and ciliated dendrites of chordotonal organs that mediate hearing and larval touch sensitivity. Mutant sperm axonemes as well as sensory neuron dendrites of Johnston's organ, the fly's auditory organ, lack dynein arms. Through deficiency mapping and sequencing candidate genes, we identified *tilB* mutations in the annotated gene CG14620. A genomic CG14620 transgene rescued deafness and male sterility of *tilB* mutants. TilB is a 395-amino-acid protein with a conserved N-terminal leucine-rich repeat region at residues 16–164 and a coiled-coil domain at residues 171–191. A *tilB*-Gal4 transgene driving fluorescently tagged TilB proteins elicits cytoplasmic expression in embryonic chordotonal organs, in Johnston's organ, and in sperm flagella. TilB does not appear to affect tubulin polyglutamylation or polyglycylation. The phenotypes and expression of *tilB* indicate function in cilia construction or maintenance, but not in intraflagellar transport. This is also consistent with phylogenetic association of *tilB* homologs with presence of genes encoding axonemal dynein arm components. Further elucidation of *tilB* functional mechanisms will provide greater understanding of cilia function and will facilitate understanding ciliary diseases.

THE cilium is a distinguishing feature of eukaryotic cells and may be coeval with the eukaryotic cell: cilia and flagella with similar form and complexity are found in unicellular microalgae and complex metazoans. Though some eukaryotic lineages lack cilia or ciliary motility, our current understanding of evolution is that these are derived states and that the most recent common ancestor of all extant eukaryotes had complex, motile cilia (Stechmann and Cavalier-Smith 2003; Cavalier-Smith 2009). Cilia are recognized by their cytoskeleton, the axoneme. In its canonical form, this is a cylinder of nine microtubule doublets, aligned with their plus ends outward. The ninefold symmetry derives from the centriole/basal body, which templates ciliary growth in interphase or postmitotic cells. Cilia are sometimes classified as motile *vs.* "primary" or sensory, on the basis of the presence (9 + 2) or absence (9 + 0) of a central microtubule pair in addition to the peripheral doublets. Indeed, most motile cilia do have a central pair, while the primary monocilia that transduce developmental and sensory stimuli lack this feature. But some 9 + 0 cilia, such as at the mammalian embryonic node, are motile. Moreover, recent findings blur the general distinction between sensory and motile cilia. For example, the flagella that propel the single-celled alga Chlamydomonas also transduce mating signals that induce cell fusion (Pan and Snell 2002), and the motile cilia that line human airway epithelia bear chemoreceptors for bitter substances (Shah *et al.* 2009).

Consistent with an ancient, monophyletic origin for cilia, a large ciliary proteome is conserved in unikonts and bikonts, the two fundamental branches of the eukaryotic evolutionary tree (Avidor-Reiss *et al.* 2004; Li *et al.* 2004). Conserved ciliary proteins include structural proteins that form the axoneme, axonemal dynein subunits that drive motility, and intraflagellar transport (IFT) particle subunits and motors. In addition, ciliary proteins that are defective in several human syndromes may have normal functions in ciliary signaling (Pan *et al.* 2005), and many more ciliary-specific proteins of unknown function suggest that other functions and activities have yet to be defined. But the multiple biological functions, highly integrated structure, and long evolutionary history of cilia can hinder a detailed understanding of ciliary mechanisms. Although many individual ciliary proteins have been

Supporting information is available online at http://www.genetics.org/cgi/content/full/genetics.110.114009/DC1.

[1]*Corresponding author:* Department of Biology, 259 Biology Bldg., University of Iowa, Iowa City, IA 52242. E-mail: daniel-eberl@uiowa.edu

identified, the individual actions of relatively few have been described. Furthermore, the diversity and variability of phenotypes that result from mutations in ubiquitous ciliary proteins—ranging from early embryonic lethality to relatively mild and partially penetrant sensory defects—are not well understood at the molecular level.

Species that bear multiple types of cilia with different functions and developmental requirements can help in the dissection of ciliary mechanisms. Drosophila construct a sperm flagellum and several types of sensory cilia: notably, the sensory cilia require IFT but the sperm flagellum does not (Han *et al.* 2003; Sarpal *et al.* 2003; Lee *et al.* 2008). Moreover, unlike vertebrates, fly development does not depend on ciliary signaling. Cilia are formed only on postmitotic sensory neurons, and mutants lacking all cilia survive to adulthood, though with severe sensorimotor defects (Dubruille *et al.* 2002). Thus, the spectrum of sperm and sensory defects in a particular mutant can help reveal the function of the affected protein. Previously, *touch-insensitive larva B* (*tilB*) mutations were found to selectively affect sperm flagella and chordotonal organs (Kernan *et al.* 1994; Eberl *et al.* 2000), auditory and vibrosensory organs in which transduction involves an active mechanical amplifier (Göpfert and Robert 2003; Göpfert *et al.* 2005). Here we identify the *tilB* gene product as a leucine-rich repeat protein and show that dynein-like arms normally present on chordotonal axonemes are missing in *tilB* mutants, suggesting a specific requirement for the TilB protein in ciliary motility and chordotonal transduction. Moreover, *tilB* is widely conserved, but only in organisms that have motile cilia or, more specifically, axonemal dyneins. In particular, the presence of a *tilB* homolog in microalgae that lack cilia but retain inner arm axonemal dyneins indicates that it is specifically required for the assembly and/or operation of the axonemal dynein arms. This supports the idea that ciliary dyneins drive mechanical amplification in the fly's ear.

MATERIALS AND METHODS

Genetic strains: Isolation of the mutant alleles $tilB^1$ and $tilB^2$ was previously described (Kernan *et al.* 1994). The *elav*-Gal4 strain was a gift of Sean Sweeney. Deficiency strains and the UAS-GFP strain were obtained from the Bloomington Drosophila Stock Center. The *tilB*-Gal4, genomic $tilB^+$ rescue strain, and all UAS or UASP constructs with tagged full-length *tilB*, or fragments thereof, are described in this study.

Transmission electron microscopy: Drosophila heads from *y w* $tilB^2$/Y mutants and *y w*/Y controls were fixed with 2.5% glutaraldehyde and 2.5% paraformaldehyde, stained with osmium tetroxide and tannic acid to visualize microtubules, and embedded in Epon resin. TEM was performed using a Hitachi H-7000 transmission electron microscope from ×10,000 to ×40,000 magnification.

Electrophysiology: The electrophysiology to record sound-evoked potentials (SEPs) was performed using the assay described previously (Eberl *et al.* 2000). Briefly, the fly is immobilized in a pipette tip. The pulse song, a component of the fly's courtship song, is played through a speaker and delivered to the fly through Tygon tubing. One electrolytically sharpened tungsten electrode is inserted in the junction between the first and second antennal segment while a second penetrates the dorsal head cuticle as a reference. The signals are subtracted with a DAM50 differential amplifier (World Precision Instruments) and then digitized and normalized using Superscope 3.0 (G. W. Instruments) software.

Deficiency mapping: Deficiency mapping of *tilB* was carried out using virgin females from balanced X chromosome deficiency lines crossed to *y w* $tilB^1$/Y67g19.1 males. The female *y w tilB*/Df progeny of the cross were examined for larval response to touch by a fine hair and scored for motility as described in the isolation of *tilB* mutants (Kernan *et al.* 1994). The deficiency map was verified by electrophysiology to determine a neuronal response to auditory stimulation. At least three flies were tested and the line was scored as noncomplementing if all three flies had no detectable electrophysiological response to the pulse song stimulus.

Sequencing: To identify the *tilB* mutant sequence changes, CG14620 was sequenced from two different PCR reactions from each of two independent DNA extractions from each of y w $tilB^1$ and y w $tilB^2$ mutant males, as well as *y w* control flies. The primers used for these PCR reactions and all other subsequent experiments are listed in supporting information, Table S1. Sequencing was performed using an ABI 3300 (Advanced Biotechnologies) machine.

Genomic rescue: A 3.5-kb genomic fragment comprising the region between the coding sequences of the flanking genes, CG14615 and CG14614, was PCR amplified and cloned into TOPO (Invitrogen, Carlsbad, CA). The fragment was then subcloned into Casper3 and sent to the Duke University Model Systems Genomics facility where it was injected into embryos for the production of transgenic lines. The genomic rescue construct was crossed into the $tilB^1$ and $tilB^2$ mutant background and electrophysiology was performed to determine whether the genomic fragment rescued the deafness phenotype.

***tilB*-Gal4 construction:** A *tilB*-Gal4 line was created by PCR amplifying the upstream intergenic regulatory region of *tilB* and cloning into TOPO (Invitrogen) between the CG14620 coding sequence and the coding sequence of CG14615, the next gene telomeric to *tilB*. The upstream regulatory region was then cloned into the Gal4 vector pPTGAL (Sharma *et al.* 2002). The entire clone was then injected into embryos to generate transgenic lines.

RT–PCR: RT–PCR was performed on RNA extracted from *y w*/Y males. The primers were designed to amplify a fragment in which the upstream primer was designed against exon 2 while the downstream primer was designed against exon 3. RNA was extracted using the Quickprep Micro mRNA purification kit (Amersham Biosciences, Piscataway, NJ). First-strand synthesis was performed using the Superscript III kit (Invitrogen). Primers used to determine expression by RT–PCR are listed in Table S1. To determine expression of Venus-tagged (V) truncations, the same procedure for RNA extraction and first-strand synthesis was used, but with different primers used for the PCR reaction as listed in Table S1.

Fusion proteins: Using primers listed in Table S1, PCR product from amplified first-strand synthesis DNA was cloned into TOPO (Invitrogen). Forward and reverse primers were designed in frame against different sites to allow for the creation of TilB truncations. The full-length and the truncated proteins differed only in the primer location for subcloning. The full-length and *tilB* truncations were then PCR amplified and cloned into the pENTR vector (Invitrogen). A recombi-

nation reaction using the Gateway Recombination System (Invitrogen) was performed that placed cDNA in frame with the protein tags. The fusion constructs were injected into embryos to create transgenics.

Immunohistochemistry: For polyglutamylation and polyglycylation assays, testes were extracted from males 1–4 days after eclosion. The tissue was fixed in 3.7% formaldehyde in phosphate-buffered saline with Tween-20 (PBST) and incubated overnight with the GT335 monoclonal primary antibody to bind polyglutamylated tubulin at a concentration of 1:500. A Texas-red conjugated rabbit anti-mouse secondary antibody was used for visualization. The antibodies Axo49 and TAPO 952 were used at a concentration of 1:500 to visualize polyglycylated tubulin, using the same Texas-red secondary antibody.

For Johnston's organ cryosections, female antennae were dissected and fixed in 4.5% paraformaldehyde. Upon cryosectioning, Texas-red conjugated phalloidin was used to visualize the actin rods of the scolopale cell. In some cases, anti-GFP primary antibody was used to visualize the GFP-tagged and the Venus-tagged fusion proteins.

RESULTS

***tilB* disrupts axoneme structure in Johnston's organ:** Two alleles of *tilB* were originally isolated in a screen for mutants that render larvae insensitive to touch (Kernan *et al.* 1994). Consistent with a role in chordotonal organs but not in other type I sensillae, *tilB* larvae also have defects in larval locomotion (Caldwell *et al.* 2003). Adult *tilB* flies have defects in motility and coordination that are less severe than those of *nomp* mutations, which affect all type I sensillae. The *tilB* mutant adults are deaf (Eberl *et al.* 2000) and lack spontaneous antenna oscillations and mechanical amplification of stimulus-induced antennal vibrations (Göpfert and Robert 2003). Chordotonal feedback is necessary to accurately generate the courtship song; thus, while *tilB* mutant males can generate courtship songs by wing vibration, their song waveform patterns are altered (Tauber and Eberl 2001). Males can mate, but are sterile because of amotile sperm (Eberl *et al.* 2000). We previously showed that *tilB* mutant sperm tail axonemes lacked the inner and other dynein arms and likely also the nexin link (Eberl *et al.* 2000). To determine whether axonemes of Johnston's organ sensory cilia have a similar phenotype we carried out electron microscopy on Johnston's organ. We examined regions of the sensory cilium proximal to the ciliary dilation where dynein arms are found (Lee *et al.* 2008). Our results show that *tilB* mutants are missing the inner and outer dynein arms in the axonemes of Johnston's organ scolopidia (Figure 1), as they are in sperm tail axonemes. However, we did not find frequent axonemal breaks and missing microtubules in Johnston's organ, as we had seen in sperm. This may be due to any of several factors that distinguish Johnston's organ axonemes from those in sperm: membrane apposition, axoneme length, and IFT dependence.

CG14620 encodes *tilB*: The *tilB* complementation group was previously mapped to the X chromosome,

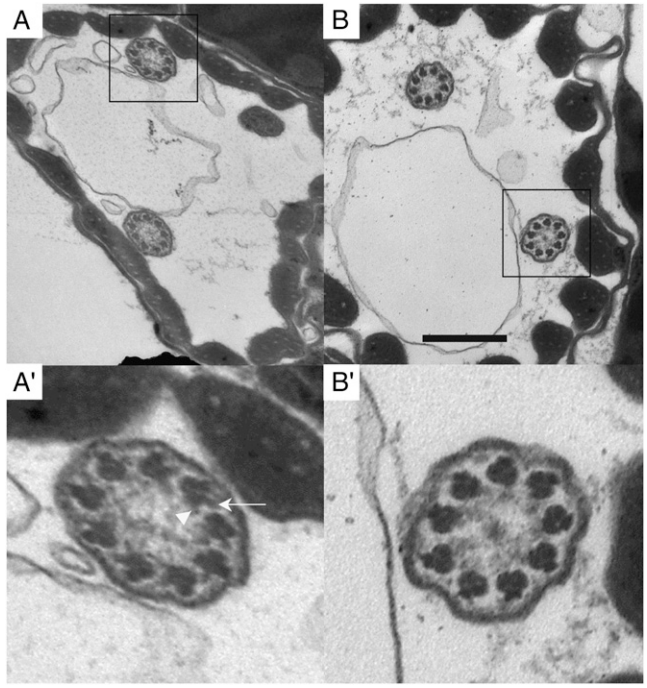

Figure 1.—Inner and outer dynein arms are lost in Johnston's organ sensory cilia of *tilB* mutants. Cross-sectional electron micrographs are shown of Johnston's organ scolopidia of a *y w* control fly (A) and a $tilB^2$ mutant (B) at the level between the basal body and the ciliary dilation, the ciliary segment that normally contains dynein arms. Enlarged views of the boxed regions of A and B are shown in A′ and B′. Outer dynein arms (arrow) and inner dynein arms (arrowhead) are present in the control but absent in $tilB^2$ flies. Bar: 500 nm.

polytene region 20A (Kernan *et al.* 1994). To refine the candidate genomic region with the goal of identifying the gene that corresponds to the *tilB* mutations, we used all available chromosomal deletions for deficiency mapping. Selected informative deficiencies are depicted in Figure 2B (see Figure 2 legend for additional details). Complementation analysis was done on the basis of larval touch sensitivity and then confirmed with electrophysiology tests for hearing. These two phenotypes gave identical results. The deficiency map places *tilB* in polytene chromosome region 20A between the genes *flamenco* (*flam*) and *wings apart* (*wap*). The only two cloned genes in this region at the time were *sluggish A* (*slgA*) and *folded gastrulation* (*fog*). The corresponding physical map covers ~972 kb and contains 48 predicted polypeptides (Figure 2A).

The annotated gene CG14620 was identified as a likely candidate gene for two reasons. First, it is the homolog of a testis factor originally found in humans and mice (Xue and Goldberg 2000). Second, expressed sequence tags from this predicted gene come from a testis cDNA library. To determine whether CG14620 corresponds to *tilB,* we sequenced the predicted exons and found mutations in CG14620 in both *tilB* alleles (Figure 2, C and D). The $tilB^1$ allele contains a

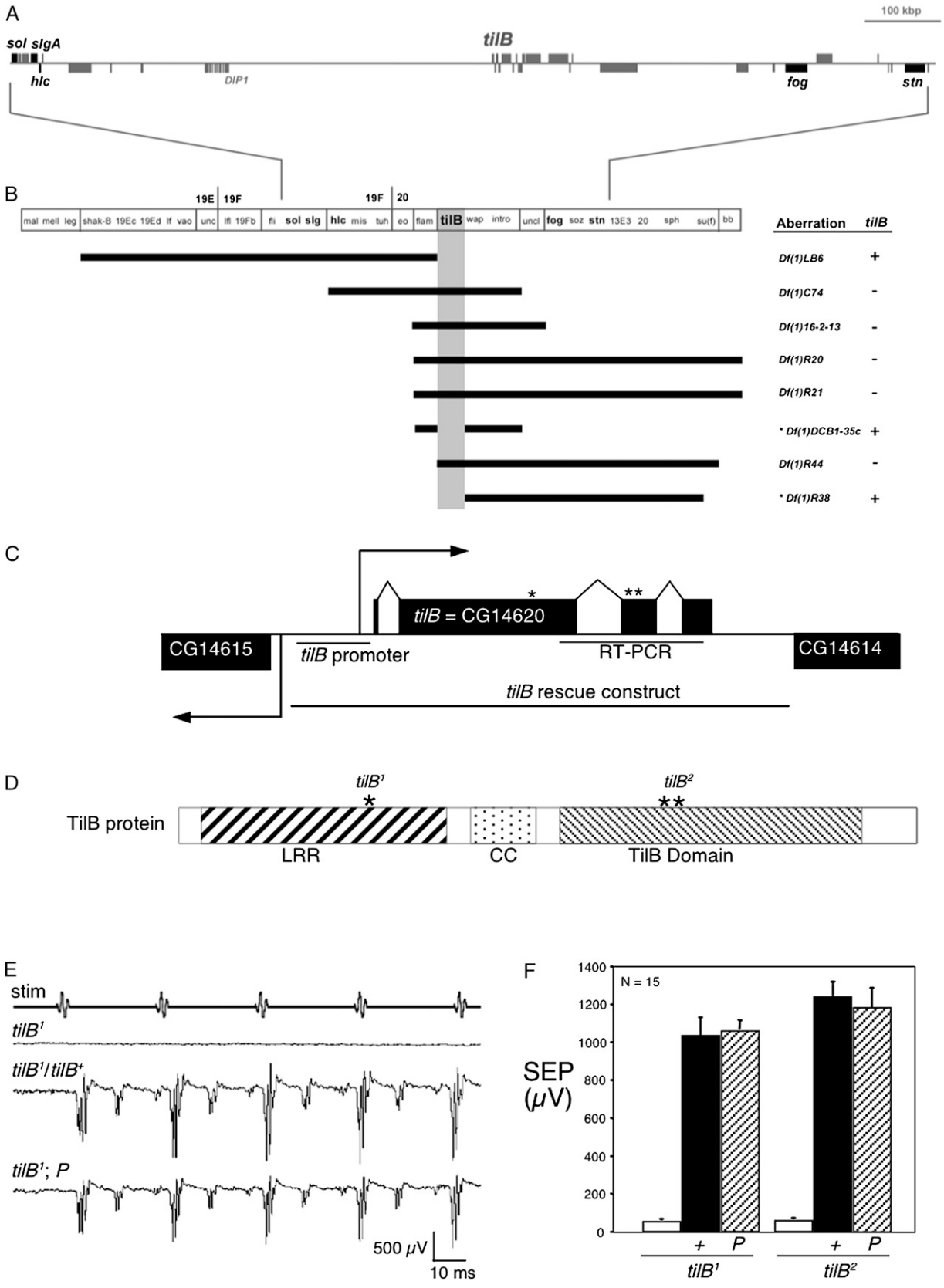

FIGURE 2.—*tilB* corresponds to CG14620 and encodes a leucine-rich repeat protein. (A) Molecular map of the 1.3-Mbp region including *tilB*. *tilB/CG14620* is located in a gene-rich cluster at the base of the X chromosome, flanked by transposon-rich intervals (transposons not indicated). Shaded bars, predicted gene spans; solid bars, molecularly and genetically identified loci. (B) Deficiency complementation map of the 19E–20B interval. Bars indicate a failure to complement. Complementation data for *tilB* are from this work; data for other loci are from FlyBase. The position of *tilB* relative to the molecularly undefined loci *wap* and *intro* is

C to T transition causing a nonsense mutation in the second exon, resulting in a truncated protein. The *tilB²* allele carries a 6-bp deletion in the third exon (Figure 2, C and D), resulting in a 2-amino-acid deletion. Neither of these two mutations was present in the premutagenesis parent chromosome (data not shown).

To confirm that CG14620 encodes the *tilB* gene, we generated a genomic rescue construct that carries CG14620 and spanned the entire region between the flanking genes, CG14615 and CG14614 (Figure 2C). SEPs were recorded from the antennal nerve of adult males carrying both the transgene and one of the *tilB* mutant alleles. The *tilB* mutants with the CG14620 genomic transgenic construct show the characteristic wild-type response to the pulse song stimulus (Figure 2E), while *tilB* mutants without the transgene lack this characteristic response. The quantification of this response indicates full rescue of the deafness phenotype from both *tilB¹* and *tilB²* mutants, using this genomic transgene (Figure 2F).

To determine whether the CG14620 genomic transgene could rescue the *tilB* mutant male sterility phenotype, we tested male sterility with ~10 males per genotype. Each male was allowed to mate with three females. Then, each female was moved to a separate vial, and all progeny in the original mating vial and in the separate vials were counted. The average progeny size for *y w tilB¹*/Y;;P{CG14620}/+ males with the genomic insertion was 305 flies, while the average progeny for *y w tilB²*/Y;;P{CG14620}/+ males was 260 adult flies. In both cases there were at least as many offspring as in *y w*/Y control males for which the average was 181 flies. Therefore the CG14620 genomic transgene can fully rescue the male sterility phenotype of both *tilB* mutants.

***tilB* is expressed in ciliated cells:** The phenotype of *tilB* mutants suggested that *tilB* should be expressed in ciliated sense organs, especially chordotonal organs, and in testes. We carried out RT–PCR using mRNA isolated from whole adults, from heads and from testes. The primers were designed to span introns (Figure 2C; Table S1) as a way to distinguish between spliced RNA and contaminating genomic DNA. Our results show that *tilB* is expressed both in the testes and in heads (Figure 3A). This is consistent with auditory and male sterility phenotypes seen in *tilB* mutants.

To confirm and refine the *tilB* expression pattern, we constructed a *tilB*-Gal4 transgenic line, which we could use to drive reporter genes and other constructs in *tilB*-expressing cells. This was produced by subcloning the entire intergenic region between *tilB* and CG14615 (Figure 2C), containing the putative *tilB* regulatory sequences, into the pPTGAL vector (Sharma *et al.* 2002). When crossed to the UAS-GFP reporter construct, *tilB*-Gal4-driven expression appears in ciliated cells, including the chordotonal organs of late stage embryos and larvae (Figure 3, B and C), neurons of Johnston's organ (Figure 3D), and femoral chordotonal organs. We found that *tilB*-Gal4 also drives expression in olfactory sensilla on the antenna, as shown with a UAS-tilB-GFP reporter (Figure 3E). In the testes, while *tilB*-Gal4 did not drive obvious expression of UAS-GFP, which is made in the standard pUAST vector (Brand and Perrimon 1993), it did drive expression in sperm when we used reporters made in the germline-compatible vector pUASP (Rorth 1998) (see below). Thus, expression of the *tilB* gene, as revealed by RT–PCR and by the *tilB*-Gal4 construct, is consistent with all the *tilB* phenotypes.

TilB protein analysis: The predicted TilB protein contains 395 amino acids (Figure 2D and Figure S1). The sequence is highly conserved in vertebrates, and clear homologs can be identified throughout eukaryotes (Figure 6). The human homolog (LRRC6) was identified as a testis-specific factor (Xue and Goldberg 2000). Analysis of the TilB protein domain structure suggests the presence of two highly conserved domains separated by a less conserved coiled-coiled region. The protein contains an N-terminal leucine-rich repeat (LRR) domain with four clear repeats from residues 16 to 107 and two additional repeats up to residue 164 that align less well with the consensus (Xue and Goldberg 2000; Morgan *et al.* 2005) (see Figure S1). Using the COILS algorithm (Lupas 1997), we see strong support for a coiled-coil segment after the LRR domain at residues 171–191 (data not shown). The remainder of the protein sequence resembles no documented motifs. However, because it is highly conserved, we define this

still unresolved, reflecting an inconsistency between the complementation patterns of *Df(1)DCB1-35c*, which deletes or disrupts *flam*, *wap*, and *intro* but not *tilB*, and *Df(1)R38*, which deletes *wap*, *intro*, and more proximal loci. In addition to the aberrations shown, *tilB* also is disrupted or deleted in *Df(1)GA22*, *Df(1)48-2*, and *Df(1)R35*; is duplicated in *Dp(1;Y)67g19.1*; and complements *Df(1)16-3-22*, *Df(1)S54*, *Df(1)17-25*, and *Df(1)JC77*. (C) The annotated gene CG14620, which lies between CG14614 and CG14615, was identified as *tilB*. The locations of sequence changes corresponding to the two alleles, *tilB¹* and *tilB²*, are shown as single and double asterisks, respectively. The genomic fragment used for transposon-mediated rescue, the upstream regulatory region used for generating *tilB*-Gal4, and the fragment used for testing expression by RT–PCR are indicated. (D) *tilB* encodes a 395-amino-acid protein. *tilB¹* changes Q171 to a stop codon and *tilB²* is an in-frame deletion removing an alanine and a tyrosine at position 313–314. The protein has three conserved domains including a leucine-rich repeat (LRR) region in the N-terminal end (residues 16–145), a central coiled-coil domain (residues 171–191), and a region that we refer to as the TilB domain (residues 202–334). (E) Rescue of hearing in *tilB* mutants with a *P*-element transgene containing the CG14620 genomic fragment, indicated in C. Representative traces are shown of sound-evoked potentials (SEPs) recorded from the antennal nerves of flies of the indicated genotypes, where *P* indicates the rescuing transgene inserted in the third chromosome. (F) Quantitative rescue of hearing in both *tilB* mutants. Flies with the P{CG14620} third chromosome transgene (indicated by *P*) have SEP amplitudes not significantly different from those of heterozygote females (indicated by +). $N = 15$ for each genotype. Error bars indicate SEM.

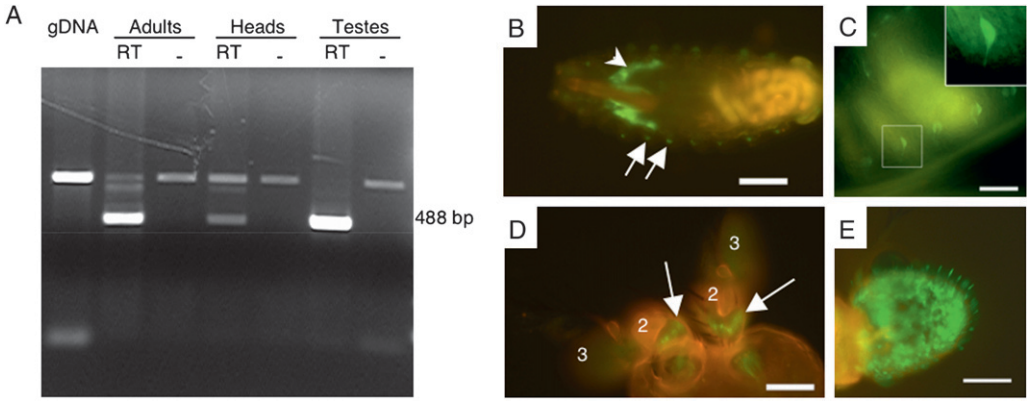

FIGURE 3.—*tilB* is expressed in ciliated cells. (A) RT–PCR of *tilB*, using primers for the fragment indicated in Fig. 2C, shows expression in the heads and testes. The expected genomic and spliced sizes are indicated. A band of the expected size is amplified from genomic DNA (gDNA). For each tissue, amplification is shown from cDNA using reverse transcriptase (RT) and from the control with this enzyme omitted (−). (B and C) Late stage embryos carrying the *tilB*-Gal4 driver and UAS-GFP show *tilB* expression in the lateral pentascolopidial organs (arrows in B). Salivary gland expression (arrowhead in B) is commonly seen in Gal4 insertion lines (BRAND and PERRIMON 1993; HRDLICKA *et al.* 2002) and therefore this expression is most likely spurious. (D) Fluorescent view of adult antennal regions shows that *tilB*-Gal4 also drives UAS-GFP expression in Johnston's organ (white arrows), which is housed within the second antennal segments (2). The third antennal segments are also indicated (3). (E) *tilB*-Gal4-driven UAS-TilB:EGFP shows expression in the olfactory sensillae of the third antennal segment. Bars: B and D, 100 μm; C and E, 50 μm.

as the TilB domain (Figure 2D). To identify other putative important functional domains, the TilB protein was analyzed by the program Scansite (scansite.mit.edu) (OBENAUER *et al.* 2003). Under conditions of high stringency we identified two potential sites of TilB phosphorylation, an SH3 site at P245 and an ERK phosphorylation site at V73. Further tests will be required to determine whether and under what conditions these sites are phosphorylated *in vivo* and their functional significance.

The mutation in $tilB^1$ is a C to T transition mutation in exon 2 that changes the CAG codon encoding a glutamine at amino acid 171 to UAG, a stop codon (Figure 2, C and D). Therefore, this allele is likely to make a truncated protein containing only the LRR domain. This is consistent with a nonfunctional protein. On the other hand, $tilB^2$ is a 6-bp deletion in exon 3, resulting in a 2-amino-acid deletion in frame with respect to the predicted coding sequence (Figure 2, C and D). This deletion removes an alanine and a tyrosine, unconserved residues 314 and 315, from the predicted amino acid sequence. While this small deletion is a much more subtle disruption of the TilB protein than the truncation of $tilB^1$, the two alleles are indistinguishable genetically.

TilB fusion proteins: To identify functional characteristics of the conserved regions of TilB, we made four truncated fusion proteins that contained the LRR region alone (LRR), the LRR region and the coiled-coil domain (LRRCC), the coiled-coil domain and the TilB domain (CCTilBD), or the TilB domain alone (TilBD). Those proteins that retained the LRR region were fused to the Myc (M) epitope tag, while those peptides that retained the TilB domain were fused to EGFP (G). (Figure 4A).

To determine that the presence of a protein tag does not disrupt protein function, we tested whether the full-length tagged version would rescue the deafness and male sterility phenotypes of the *tilB* mutants. Indeed the full-length N-terminal Myc-tagged and C-terminal GFP-tagged proteins rescue deafness of both *tilB* mutant alleles (Figure 4B). Therefore, neither of the tags significantly interferes with TilB function in Johnston's organ. Importantly, there is also no discernible difference in hearing between flies with and without the *tilB*-Gal4 driver, indicating that the very low level of TilB protein expression, allowed by slight leakiness of the UAS sequences, is sufficient for rescue. However, male sterility of neither *tilB* mutant allele was rescued by driving UAS-M:TilB or UAS-TilB:G with the *tilB*-Gal4 driver (data not shown). As described below, this is most likely attributable to the incompatibility of the standard UAS vector with germline expression (RORTH 1998).

While the full-length tagged TilB proteins are able to rescue the auditory defects of *tilB* mutants, none of the truncations rescued $tilB^2$ deafness (Figure 4B). This indicates that all domains of the protein are necessary for the function of TilB in Johnston's organ. Two major possible explanations for the failure of the truncations to rescue are that the truncated fusion proteins are not expressed or that they are unable to localize properly in the cell. To distinguish these possibilities, we examined the expression of the GFP-tagged fusions in chordotonal organs. Fusion protein expression was driven in the neurons using the pan-neuronal driver *elav*-Gal4 for better visualization of the TilB protein, which has low expression. In the chordotonal organs of the embryonic body wall, not only the full-length TilB:G, but also the truncated proteins were expressed (Figure 4, C–E). In each case, the protein is present throughout the cytoplasm, including in the inner and outer dendritic segments. In the adult Johnston's organ, we see a similar pattern of expression (Figure 4, G–I) throughout the neuronal cytoplasm. Localization of the TilB full-length

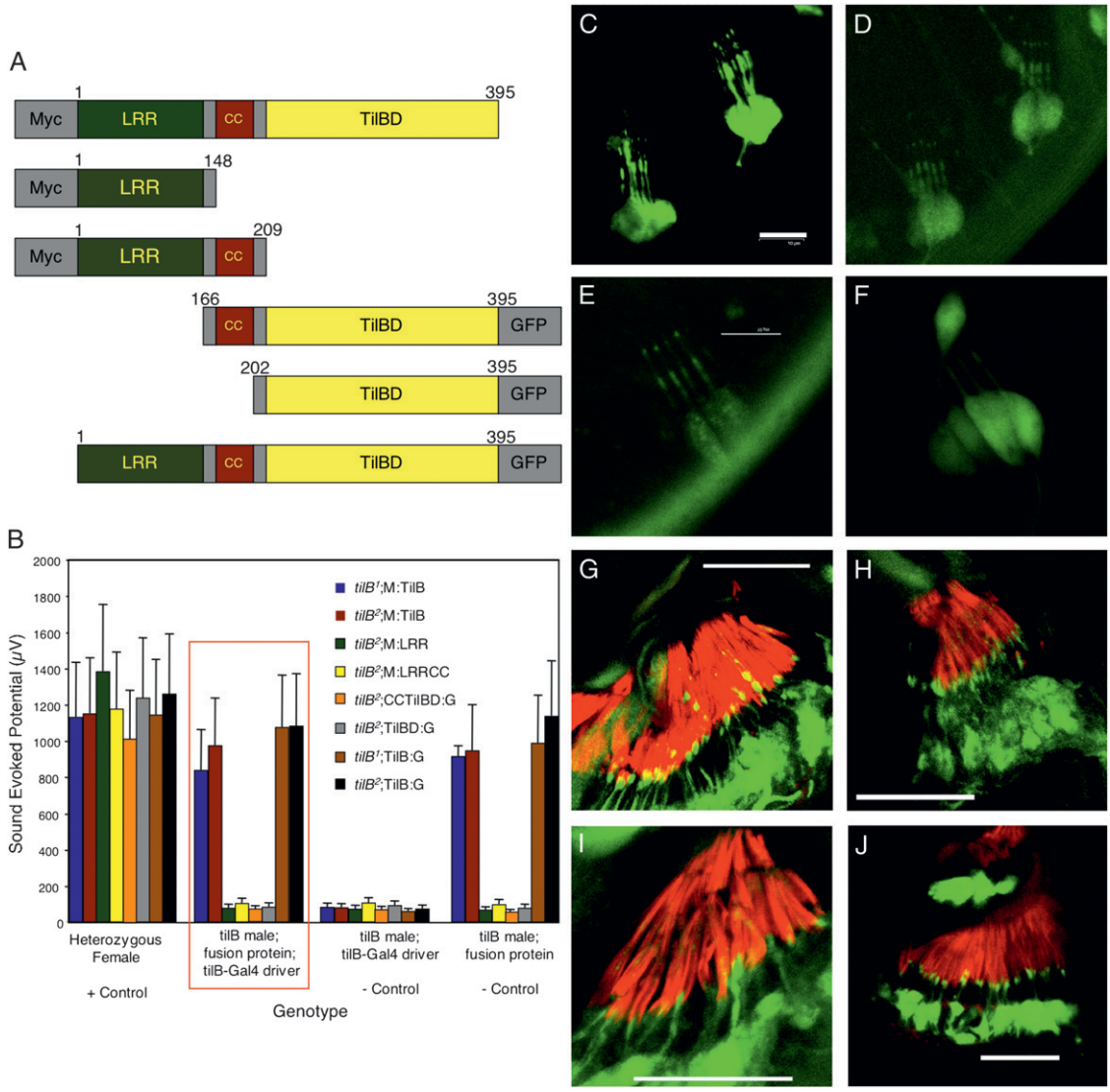

FIGURE 4.—TilB fusion proteins rescue hearing and are present in chordotonal neuronal cell bodies and dendrites. (A) Two full-length and four truncated fusion proteins were constructed that contain the leucine-rich repeat region (LRR) alone, the LRR and coiled-coil domain (CC), the CC together with the TilB domain (CCTilBD), or the TilB domain alone (TilBD). Those polypeptides that retained the N-terminal LRR region were tagged with Myc (M), while those that retained the C-terminal TilB domain were tagged with GFP (G). (B) Electrophysiology shows that the full-length M:TilB and TilB:G fusions rescue hearing in *tilB*^{1} and *tilB*^{2} mutants (red box). The full-length fusion proteins rescue without the *tilB*-Gal4 driver, indicating that a low level of protein allowed by the UAS sequences is sufficient for rescue. Each bar in the graph depicts the mean + SEM, with $N = 15$. (C–F) Expression of GFP fusion proteins in embryonic lch5 organs with the *tilB*-Gal4 driver. (C) The full-length TilB:G fusion protein is present throughout the cytoplasm including the inner and outer dendritic segments. (D) The CC-TilBD:G fusion is similarly distributed, as are the TilBD:G (E) and free GFP alone (F). (G–J) Johnston's organ expression of the same constructs as in C–F with the *elav*-Gal4 driver, counterstained with phalloidin (red). Arrowheads indicate the basal body region at the junction of the inner and outer dendritic segments, while arrows point to the ciliary dilations. Bar in C: 10 μm for C–F. Bars in G–J: 25 μm.

and truncated proteins in chordotonal neurons is not substantially different from that of free GFP (Figure 4, F and J), suggesting that there is no obvious trafficking of the protein, for example, to the ciliary axoneme, as might be expected if TilB were an axonemal structural component. There is a tendency for the fluorescence of the truncated proteins to be lower than that of the full-length TilB protein, suggesting a possible loss of protein stability; however, analysis of many different chromosomal locations for each transgene construct, or all constructs targeted to the same insertion site, would be required to provide confidence for an effect on stability. Finally, distribution of the full-length TilB protein when driven by *tilB*-Gal4 is also similar, though less intense (Figure 5B). Given the ability of the full-length fusion proteins to rescue hearing in the *tilB* mutants, it is possible that even the expression levels driven by *tilB*-Gal4 are saturating and that the broad expression in the cytoplasm is an artifact of overexpression. To address this, we examined the UAS-TilB:G flies without driver,

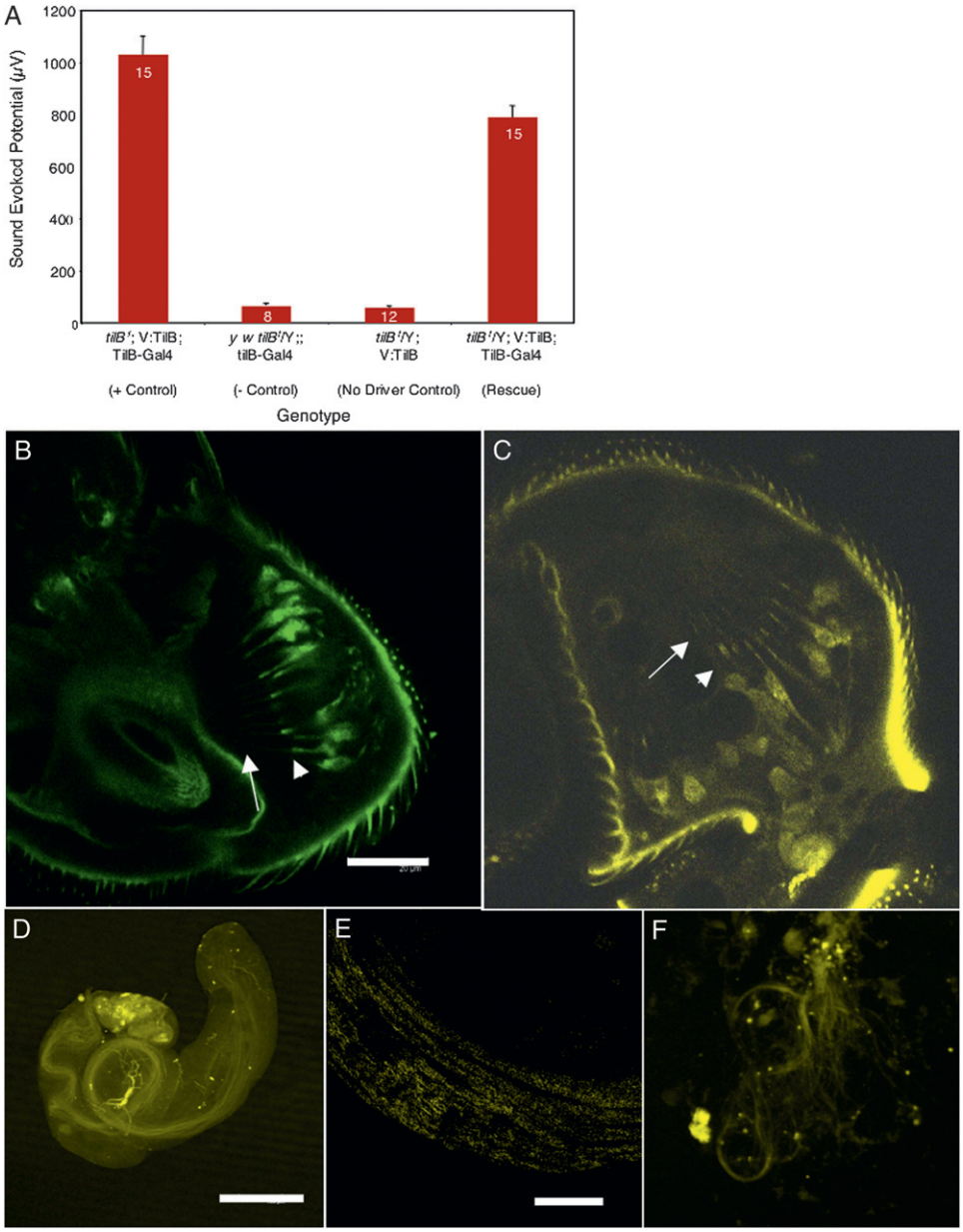

FIGURE 5.—Expression of TilB with a germline-compatible vector. (A) An N-terminal Venus (EYFP)-tagged TilB fusion protein generated in the pUASP vector rescues deafness only in the presence of a Gal4 driver. Flies with the driver but without V:TilB are deaf, as are flies with V:TilB but without the driver. This is in contrast to TilB:G, which rescues deafness even in the absence of the driver. (B and C) To ensure that overexpression of full-length TilB fusion proteins did not saturate the cell, the full-length fusion proteins were expressed under the control of the *tilB*-Gal4 driver. The results still show that the protein is present in the inner dendritic segment and basal body (arrowheads). V:TilB and TilB:G were also present in the outer dendritic segment (arrows). Bars: 20 μm. (D) Transgenic flies with V:TilB created using the pUASP vector show TilB localization to the sperm flagella when driven by *tilB*-Gal4. (E) V:TilB showing presence in testes. Bar: 200 μm. E shows V:TilB in sperm bundle in testes and F shows V:TilB in sperm released from testes. Bars in E and F: 50 μm.

but were unable to detect GFP fluorescence (not shown). Nevertheless, further experiments with UASp-Venus-TilB, described below, suggest that cytoplasmic localization of the TilB protein is likely correct.

To address the failure of the UAS-mediated expression in testes and rescue of male fertility, we generated a TilB fusion construct with an N-terminal EYFP "Venus" (V) tag, using the pUASP vector that had been developed to obtain germline expression (RORTH 1998). Again to confirm function, we tested the V:TilB fusion proteins for hearing and male sterility rescue (Figure 5A). Electrophysiology of flies expressing V:TilB fusion proteins driven by *tilB*-Gal4 in a *tilB* mutant background shows a strong sound-evoked potential in response to the pulse song (Figure 5A). However, in contrast to the full-length TilB constructs tagged with Myc or GFP made in the UAS vector, rescue of hearing with V:TilB was significantly less than complete, only ~75% of controls (*t*-test: $P < 0.01$, two-tailed). Furthermore, again in contrast to the TilB:G construct, V:TilB does not rescue *tilB* in the absence of a driver. This most likely reflects a lower expression level than that of UAS-TilB:G even under *tilB*-Gal4 control (Figure 5B). The cellular pattern on V:TilB is consistent with localization throughout the cytoplasm, including the inner and outer dendritic compartments.

V:TilB under control of *tilB*-Gal4 does not rescue male sterility (0 progeny among 10 males) and in a testis squash from these flies, the sperm are nonmotile (data not shown). Nevertheless, we see expression of V:TilB in the sperm (Figure 5, D–F). This expression is visible in the intact testis at low magnification (Figure 5D) and at

high magnification (Figure 5E) and is retained in the individual sperm tails after disruption of the testis in a squash preparation (Figure 5F). The inability to rescue male sterility in light of germline expression is consistent with the possibility that the N-terminal fusion disrupts protein function in an alternative structural environment such as the sperm tail in comparison to the Johnston's organ. An alternative explanation would be that TilB function in sperm tail is sensitive to the delayed transcription of Gal4/UAS constructs when compared to endogenous *tilB* or genomic rescue constructs.

N-terminal fusion proteins VLRR and VLRRCC were also produced. However, these proteins were undetectable by fluorescence in testes, the Johnston's organ, or late stage embryos using *elav*-Gal4 or *tilB*-Gal4 drivers (data not shown). Using RT–PCR on whole fly mRNA, we were easily able to detect the transcripts of these truncated fusion proteins (data not shown), suggesting that TilBD may be necessary for stability.

Tubulin polyglutamylation and polyglycylation are not lost in *tilB* mutants: There were several reasons to suspect that *tilB* could be involved in polyglutamylation or polyglycylation of axonemal tubulins. First, one of the five proteins shown to be involved in polyglutamylation of tubulin, PGS4, was found to have an N-terminal leucine-rich repeat region (Janke *et al.* 2005). Second, polyglutamylation and polyglycylation are necessary for the proper movement of sea urchin sperm (Gagnon *et al.* 1996). Third, tubulins in Drosophila sperm are reported to be polyglutamylated and polyglycylated (Bressac *et al.* 1995; Bré *et al.* 1996). Fourth, the *tilB* sperm defects are similar to sperm defects caused by mutations in the β-tubulin C-terminal region (Nielsen *et al.* 2001; Popodi *et al.* 2005). These data show disruptions of the axoneme and loss of inner and outer dynein arms similar to those we see in *tilB*. Interestingly, it is the C-terminal ends of α- and β-tubulins that are polyglutamylated and polyglycylated.

To directly test whether polyglycylation or polyglutamylation is affected in *tilB* mutant sperm, we used antibodies that specifically recognized these modifications. The data show that both polyglycylation and polyglutamylation occur in the sperm of both *tilB* mutants and *y w* males. Because both modifications are present in *tilB* mutant testes (Figure S2), we cannot conclude that TilB has any functional role in tubulin polyglutamylation or polyglycylation.

DISCUSSION

The human *tilB* ortholog, LRRC6, also called **l**eucine-**r**ich **t**estes **p**rotein (LRTP), is expressed in midpachytene spermatocytes, while immunohistochemistry shows LRTP most abundant during pachytene and diplotene cells, consistent with a role in meiosis (Xue and Goldberg 2000). In Trypanosoma, the *tilB* ortholog (***T**rypanosoma **b**rucei* **l**eucine-**r**ich **t**estes **p**rotein, TbLRTP) associates with the basal body (Morgan *et al.* 2005). RNAi against the trypanosome TbLRTP results in basal body duplications and thereby increases the flagellar number. The authors also suggest that TbLRTP is necessary for cell cycle regulation because the size of the parasites correlates with TbLRTP overexpression and RNAi knockdown.

In zebrafish, the *tilB* ortholog *seahorse* (*sea*) was first identified in a screen for polycystic kidney disease mutants (Sun *et al.* 2004), which typically are associated with ciliary defects. More recently, *sea* was identified in the hair cell transcriptome (McDermott *et al.* 2007) and the hair cell kinocilia in the semicircular canal cristae were swollen near the base in *sea* mutants. The Sea protein is expressed in ciliated tissues such as Küpffer's vesicle, where it is localized to cytoplasmic puncta, and is required for ciliary function, though not for ciliary assembly or motility (Kishimoto *et al.* 2008). However, characterization of two additional *sea* alleles, in comparison to splice-site morpholino studies, suggested that *sea* does affect ciliary motility, that the alleles are hypomorphic, and that there is likely to be a maternal effect (Serluca *et al.* 2009).

Like the zebrafish ortholog, the TilB protein in Drosophila is associated with ciliary function. However, TilB differs from its trypanosome and zebrafish orthologs in its cellular localization throughout the cytoplasm instead of being restricted to the basal bodies or to cytoplasmic puncta. Furthermore, TilB also differs in its phenotypic effect on axonemal structure with loss of axonemal dynein arms both in sperm flagella and in Johnston's organ sensory cilia. These more drastic phenotypic effects are reflected in loss of sperm motility. Our data do not support a meiotic role for TilB. Differences from the trypanosome could arise from differences in protein structure, as the TbLRTP protein lacks ~25 residues present in the fly and vertebrate proteins. The zebrafish *sea* mutant phenotype may be less severe than that of the fly if the *sea* mutations are not completely null, as at least the point mutations suggest, and also if there is a maternal contribution from the heterozygous mothers.

The absence of axonemal components suggests that TilB either is an integral component of the axoneme or is needed to preassemble or transport the dynein arms to the axoneme. Our data, suggesting that the TilB protein is not specifically localized to the cilium, favor a preassembly or transport function. In Chlamydomonas, outer dynein arms are preassembled at the basal body and transported to the axoneme by intraflagellar transport (Fowkes and Mitchell 1998; Hou *et al.* 2007). While TilB is not an intraflagellar transport protein, TilB could be a chaperone protein necessary for properly localized, preassembled inner and outer dynein arm complexes. Indeed, the distribution of TilB/LRRC6 orthologs across the eukaryotic evolutionary

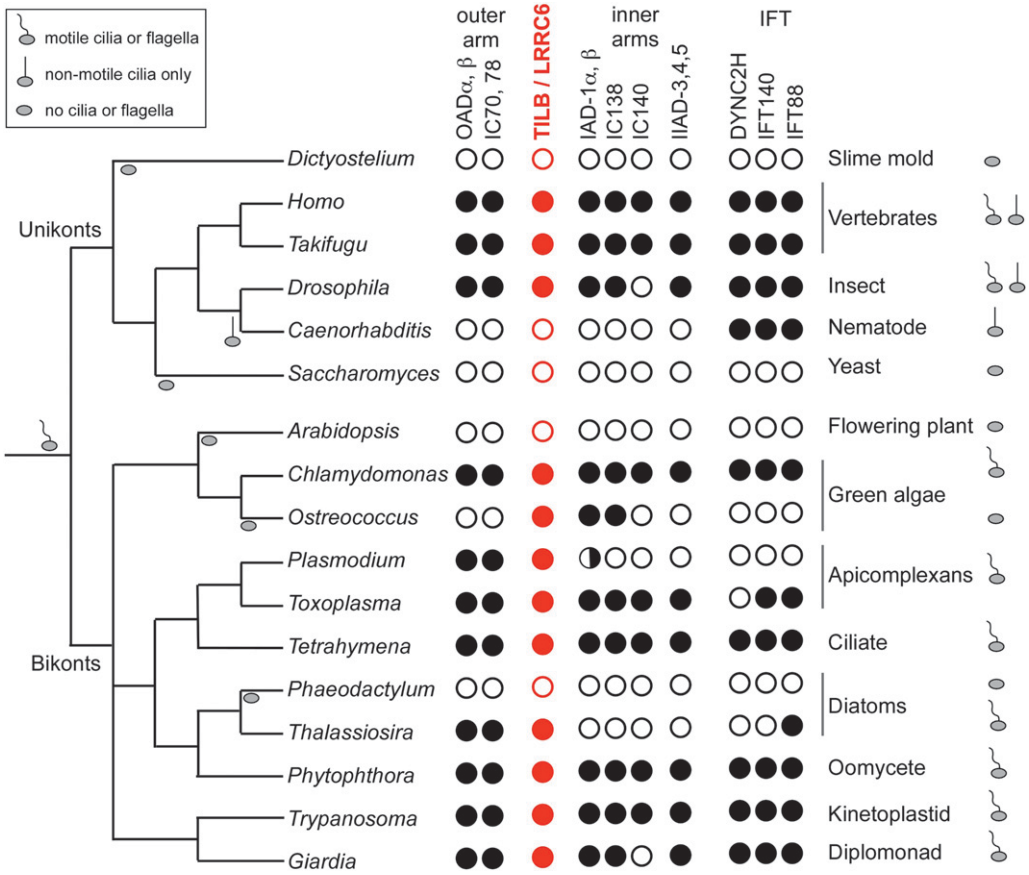

FIGURE 6.—*tilB* is conserved in ciliated eukaryotes and co-occurs with axonemal dyneins. This figure is based on Figure 4 of WICKSTEAD and GULL (2007); data in black are from that work. Columns indicate proteins representing axonemal dynein subunits, including dynein heavy chains (DHC) and intermediate chains (IC) from the outer (ODA) and inner (IDA) dynein arms, and from the intraflagellar transport (IFT) pathway, including the IFT dynein (DYNCH2). Rows list representative unikont and bikont eukaryotes with sequenced genomes. Each solid circle indicates a *tilB* ortholog in that species, as determined by the top score in reciprocal BLASTP or TBLASTN searches. Open circle: no homolog present. TilB orthologs, accession numbers, and *E*-values are as follows: Homo, *Homo sapiens* testis-specific leucine-rich repeat protein (LRRC6; AAB02976), 8*e*-80; Takifugu, *Takifugu rubripes* (Ensembl release 56) scaffold 3605, 4*e*-40 (partial); Chlamydomonas, *Chlamydomonas reinhardtii* protein ID 107408, 8*e*-37 (partial); Ostreococcus, *Ostreococcus lucimarinus* ABO94938.1, 3*e*-53 and *O. tauri* CAL52896.1, 1*e*-52; Plasmodium, *Plasmodium knowlesii*, CAQ42230.1, 4*e*-50; Toxoplasma, *Toxoplasma gondii* EEA99420.1, 2*e*-44; Tetrahymena, *Tetrahymena thermophila* EAR92110.1, 4*e*-60; Thalassiosira, *Thalassiosira pseudonana* EED89058.1, 3*e*-45; Phythopthora, *Phythopthora sojae* scaffold 12 90634-90933, 1*e*-32; Trypanosoma, *Trypanosoma brucei* AAX80642.1, 9*e*-55; Giardia, *Giardia intestinalis* EET00698, 3*e*-43.

tree also supports a specific role in the assembly or operation of axonemal dynein arms (Figure 6). As expected, *tilB* orthologs are found in almost all ciliated cells but not in nonciliated lineages such as fungi and flowering plants. But the exceptions to this general rule are instructive. Nematodes, which have only nonmotile sensory cilia (WRIGHT 1983; QUARMBY and LEROUX 2010) and lack axonemal dyneins (Figure 6), also lack a *tilB* homolog. Conversely, well-conserved *tilB* homologs are present in both sequenced species of the marine microalga Ostreococcus (*Ostreococcus lucimarinus* and *O. tauri*). These tiny (1-μm diameter) unicellular algae have no known flagellated phase and lack the entire IFT system and most axonemal dynein subunits. But they have retained one set of axonemal dynein proteins: IAD1 inner arm heavy chains and the associated IC138 intermediate chain (WICKSTEAD and GULL 2007). This, the only known case of axonemal dyneins being retained without an axoneme, suggests a requirement for TilB in the assembly or function of inner arm dyneins, independent of any axonemal function. A *tilB* ortholog is also found in the marine diatom Thalassiosira, which has motile cilia bearing only the outer dynein arms; the inner arms and all their protein subunits are absent (WICKSTEAD and GULL 2007). Therefore, TilB may be required for the assembly of any axonemal dynein.

The very specific loss of dynein arms in the context of otherwise normal ciliary structure in the Johnston's organ of *tilB* mutant flies suggests that the role of the cilium in hearing includes active ciliary movement. The dendritic tips are firmly attached to the extracellular matrix comprising the dendritic caps. Thus, the mechanical signal propagated from acoustically activated aristae must reach the sensory dendrite. However, because *tilB* mutants lack the normal spontaneous oscillation of the antenna and nonlinear mechanics under acoustic stimulation (GÖPFERT and ROBERT 2003; GÖPFERT *et al.* 2005; ALBERT *et al.* 2007; NADROWSKI *et al.* 2008), it is likely that the dynein arms are required for these functions (KERNAN 2007). We recently showed that the Drosophila RempA protein, homologous to Chlamydomonas IFT122, localizes specifically to the chordotonal ciliary dilation, which we propose delimits

the chordotonal cilium into a long proximal motile segment dependent on dynein arm function and a distal nonmotile sensory segment (Lee *et al.* 2008). While our data are most consistent with TilB acting in preassembly or transport of dynein arm complexes, we cannot rule out the possibility that TilB also plays a role in preassembly or trafficking of mechanotransduction complexes.

We are grateful to Sean Sweeney for providing *elav*-Gal4 fly stocks and the Bloomington Stock Center for deficiency stocks. We thank Dean Abel for electron microscopy, the Department of Biology for providing EM preparatory facilities, and the University of Iowa Central Microscopy Research Facility for use of the electron microscopes used in this study. We thank Marie-Helen Bré for anti-polyglycylated tubulin antibodies and Carsten Janke for the GT335 antibody. DNA sequencing was conducted at the Roy J. Carver Center for Comparative Genomics at the University of Iowa. This research was supported by National Institutes of Health (NIH) grants DC004848 to D.F.E. and DC002780 to M.J.K. R.G.K. was partially supported by the NIH Pre-Doctoral Training Program in Genetics T32 grant GM008629.

LITERATURE CITED

Albert, J. T., B. Nadrowski and M. C. Göpfert, 2007 Mechanical signatures of transducer gating in the *Drosophila* ear. Curr. Biol. **17:** 1000–1006.

Avidor-Reiss, T., A. M. Maer, E. Koundakjian, A. Polyanovsky, T. Keil *et al.*, 2004 Decoding cilia function: defining specialized genes required for compartmentalized cilia biogenesis. Cell **117:** 527–539.

Brand, A. H., and N. Perrimon, 1993 Targeted gene expression as a means of altering cell fates and generating dominant phenotypes. Development **118:** 401–415.

Bré, M. H., V. Redeker, M. Quibell, J. Darmanaden-Delorme, C. Bressac *et al.*, 1996 Axonemal tubulin polyglycylation probed with two monoclonal antibodies: widespread evolutionary distribution, appearance during spermatozoan maturation and possible function in motility. J. Cell Sci. **109**(Pt. 4): 727–738.

Bressac, C., M. H. Bré, J. Darmanaden-Delorme, M. Laurent, N. Levilliers *et al.*, 1995 A massive new posttranslational modification occurs on axonemal tubulin at the final step of spermatogenesis in Drosophila. Eur. J. Cell Biol. **67:** 346–355.

Caldwell, J. C., M. M. Miller, S. Wing, D. R. Soll and D. F. Eberl, 2003 Dynamic analysis of larval locomotion in *Drosophila* chordotonal organ mutants. Proc. Natl. Acad. Sci. USA **100:** 16053–16058.

Cavalier-Smith, T., 2009 Deep phylogeny, ancestral groups and the four ages of life. Philos. Trans. R. Soc. Lond. B **365:** 111–132.

Dubruille, R., A. Laurençon, C. Vandaele, E. Shishido, M. Coulon-Bublex *et al.*, 2002 *Drosophila* regulatory factor X is necessary for ciliated sensory neuron differentiation. Development **129:** 5487–5498.

Eberl, D. F., R. W. Hardy and M. Kernan, 2000 Genetically similar transduction mechanisms for touch and hearing in *Drosophila*. J. Neurosci. **20:** 5981–5988.

Fowkes, M. E., and D. R. Mitchell, 1998 The role of preassembled cytoplasmic complexes in assembly of flagellar dynein subunits. Mol. Biol. Cell **9:** 2337–2347.

Gagnon, C., D. White, J. Cosson, P. Huitorel, B. Eddé *et al.*, 1996 The polyglutamylated lateral chain of alpha-tubulin plays a key role in flagellar motility. J. Cell Sci. **109:** 1545–1553.

Göpfert, M. C., and D. Robert, 2003 Motion generation by *Drosophila* mechanosensory neurons. Proc. Natl. Acad. Sci. USA **100:** 5514–5519.

Göpfert, M. C., A. D. L. Humphris, J. T. Albert, D. Robert and O. Hendrich, 2005 Power gain exhibited by motile mechanosensory neurons in *Drosophila* ears. Proc. Natl. Acad. Sci. USA **102:** 325–330.

Han, Y.-G., B. H. Kwok and M. J. Kernan, 2003 Intraflagellar transport is required in *Drosophila* to differentiate sensory cilia but not sperm. Curr. Biol. **13:** 1679–1686.

Hou, Y., H. Qin, J. A. Follit, G. J. Pazour, J. L. Rosenbaum *et al.*, 2007 Functional analysis of an individual IFT protein: IFT46 is required for transport of outer dynein arms into flagella. J. Cell Biol. **176:** 653–665.

Hrdlicka, L., M. Gibson, A. Kiger, C. Micchelli, M. Schober *et al.*, 2002 Analysis of twenty-four Gal4 lines in *Drosophila melanogaster*. Genesis **34:** 51–57.

Janke, C., K. Rogowski, D. Wloga, C. Regnard, A. V. Kajava *et al.*, 2005 Tubulin polyglutamylase enzymes are members of the TTL domain protein family. Science **308:** 1758–1762.

Kernan, M. J., 2007 Mechanotransduction and auditory transduction in *Drosophila*. Pflügers Arch. **454:** 703–720.

Kernan, M., D. Cowan and C. Zuker, 1994 Genetic dissection of mechanosensory transduction: mechanoreception-defective mutations of Drosophila. Neuron **12:** 1195–1206.

Kishimoto, N., Y. Cao, A. Park and Z. Sun, 2008 Cystic kidney gene *seahorse* regulates cilia-mediated processes and Wnt pathways. Dev. Cell **14:** 954–961.

Lee, E., E. Sivan-Loukianova, D. F. Eberl and M. J. Kernan, 2008 An IFT-A protein is required to delimit functionally distinct zones in mechanosensory cilia. Curr. Biol. **18:** 1899–1906.

Li, J. B., J. M. Gerdes, C. J. Haycraft, Y. Fan, T. M. Teslovich *et al.*, 2004 Comparative genomics identifies a flagellar and basal body proteome that includes the BBS5 human disease gene. Cell **117:** 541–552.

Lupas, A., 1997 Predicting coiled-coil regions in proteins. Curr. Opin. Struct. Biol. **7:** 388–393.

McDermott, Jr., B. M., J. M. Baucom and A. J. Hudspeth, 2007 Analysis and functional evaluation of the hair-cell transcriptome. Proc. Natl. Acad. Sci. USA **104:** 11820–11825.

Morgan, G. W., P. W. Denny, S. Vaughan, D. Goulding, T. R. Jeffries *et al.*, 2005 An evolutionary conserved coiled-coil protein implicated in polycystic kidney disease is involved in basal body duplication and flagellar biogenesis in *Trypanosoma brucei*. Mol. Cell. Biol. **25:** 3774–3784.

Nadrowski, B., J. T. Albert and M. C. Göpfert, 2008 Transducer-based force generation explains active process in *Drosophila* hearing. Curr. Biol. **18:** 1365–1372.

Nielsen, M. G., F. R. Turner, J. A. Hutchens and E. C. Raff, 2001 Axoneme-specific b-tubulin specialization: a conserved C-terminal motif specifies the central pair. Curr. Biol. **11:** 529–533.

Obenauer, J. C., L. C. Cantley and M. B. Yaffe, 2003 Scansite 2.0: proteome-wide prediction of cell signaling interactions using short sequence motifs. Nucleic Acids Res. **31:** 3635–3641.

Pan, J., and W. J. Snell, 2002 Kinesin-II is required for flagellar sensory transduction during fertilization in *Chlamydomonas*. Mol. Biol. Cell **13:** 1417–1426.

Pan, J., Q. Wang and W. J. Snell, 2005 Cilium-generated signaling and cilia-related disorders. Lab. Invest. **85:** 452–463.

Popodi, E. M., H. D. Hoyle, F. R. Turner and E. C. Raff, 2005 The proximal region of the β-tubulin C-terminal tail is sufficient for axoneme assembly. Cell Motil. Cytoskeleton **62:** 48–64.

Quarmby, L. M., and M. R. Leroux, 2010 Sensorium: The original *raison d'être* of the motile cilium? J. Mol. Cell Biol. **2:** 65–67.

Rorth, P., 1998 Gal4 in the Drosophila female germline. Mech. Dev. **78:** 113–118.

Sarpal, R., S. V. Todi, E. Sivan-Loukianova, S. Shirolikar, N. Subramanyan *et al.*, 2003 The *Drosophila* kinesin associated protein (DmKAP) interacts with the Kinesin II motor subunit Klp64D to assemble chordotonal organ sensory cilia but not sperm tails. Curr. Biol. **13:** 1687–1696.

Serluca, F. C., B. Xu, N. Okabe, K. Baker, S.-Y. Lin *et al.*, 2009 Mutations in zebrafish leucine-rich repeat-containing six-like affect cilia motility and result in pronephric cysts, but have variable effects on left-right patterning. Development **136:** 1621–1631.

Shah, A. S., Y. Ben-Shahar, T. O. Moninger, J. N. Kline and M. J. Welsh, 2009 Motile cilia of human airway epithelia are chemosensory. Science **325:** 1131–1134.

Sharma, Y., U. Cheung, E. W. Larsen and D. F. Eberl, 2002 pPTGAL, a convenient Gal4 P-element vector for testing expression of enhancer fragments in *Drosophila*. Genesis **34:** 115–118.

Stechmann, A., and T. Cavalier-Smith, 2003 The root of the eukaryote tree pinpointed. Curr. Biol. **13:** R665–R666.

Sun, Z., A. Amsterdam, G. J. Pazour, D. G. Cole, M. S. Miller *et al.*, 2004 A genetic screen in zebrafish identifies cilia genes as a principal cause of cystic kidney. Development **131:** 4085–4093.

Tauber, E., and D. F. Eberl, 2001 Song production in auditory mutants of *Drosophila*: the role of sensory feedback. J. Comp. Physiol. A **187:** 341–348.

Wickstead, B., and K. Gull, 2007 Dyneins across eukaryotes: a comparative genomic analysis. Traffic **8:** 1708–1721.

Wright, K. A., 1983 Nematode chemosensilla: form and function. J. Nematol. **15:** 151–158.

Xue, J. C., and E. Goldberg, 2000 Identification of a novel testis-specific leucine-rich protein in humans and mice. Biol. Reprod. **62:** 1278–1284.

Communicating editor: T. C. Kaufman

GENETICS

Supporting Information
http://www.genetics.org/cgi/content/full/genetics.109.114009/DC1

Hearing in Drosophila Requires TilB, a Conserved Protein Associated With Ciliary Motility

Ryan G. Kavlie, Maurice J. Kernan and Daniel F. Eberl

DOI: 10.1534/genetics.109.114009

A.

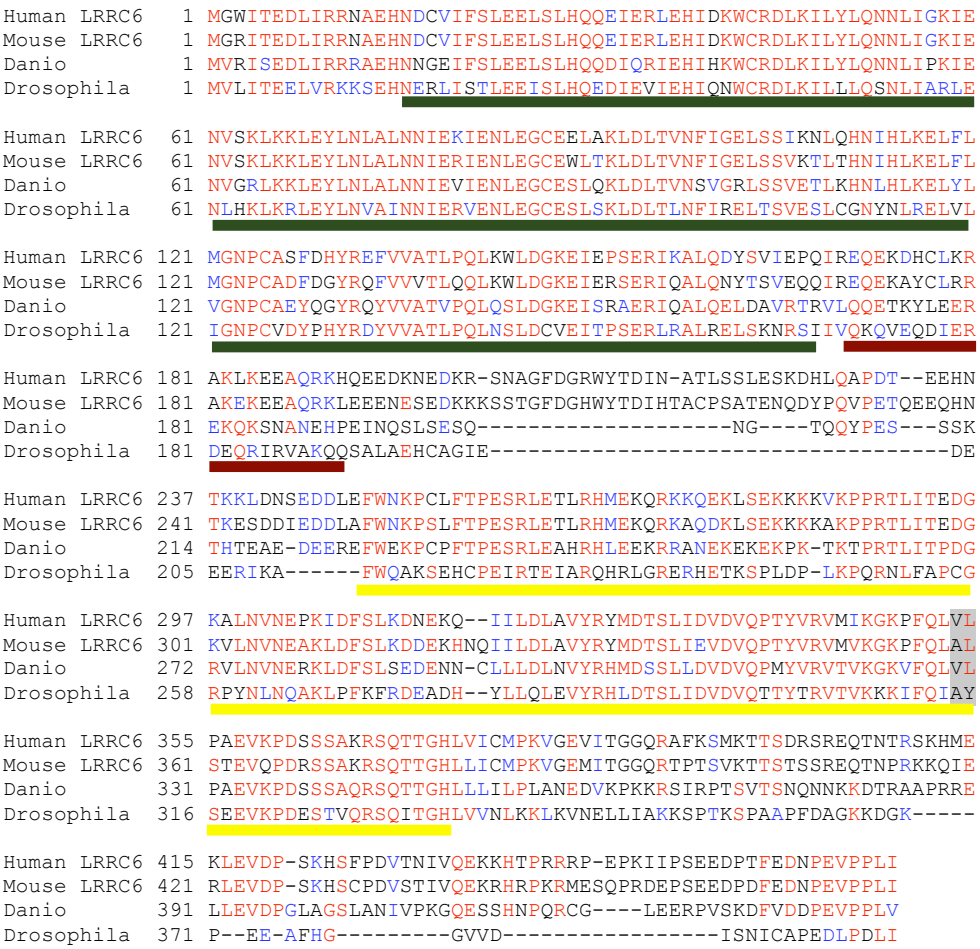

B.

```
Cons  LXXLXXIXLXXNXIXXIXXLXX

 16   ISTLEEISLHQEDIEVIEHIQNW
 39   CRDLKILLLQSNLIARLENLHK
 61   LKRLEYLNVAINNIERVENLEG
 83   CESLSKLDLTLNFIRELTSVESLCQ
108   NYNLRELVLIGNPCV / 12 / LPQ
138   LNSLDCVEITPSERLRALRELSKNRSI
```

FIGURE S1.—TilB protein structure. A) ClustalW alignment of TilB and its human, mouse, and zebrafish homologues. The alignment shows high conservation of TilB and its homologs from vertebrates to humans. Red = identities, Blue = similarities. The amino acids underlined in green constitute the leucine-rich-repeat region. The amino acids underlined in burgundy comprise the coiled-coil region. The region underlined in yellow is the TilB domain. The amino acids shaded in gray are those deleted by the *tilB*^{2} 6bp deletion mutation. Accession numbers used in this analysis: *Drosophila melanogaster* NP_608460.1, *Homo sapiens* NP_036604.2, *Mus musculus* NP_062330.1, and *Danio rerio* NP_001002311.1. B) TilB Leucine-rich repeats. LRR consensus of the SDS22 class is shown, along with an alignment of the six LRRs of the TilB protein. In repeat 5, there are 12 residues that do not appear to fit the LRR structure.

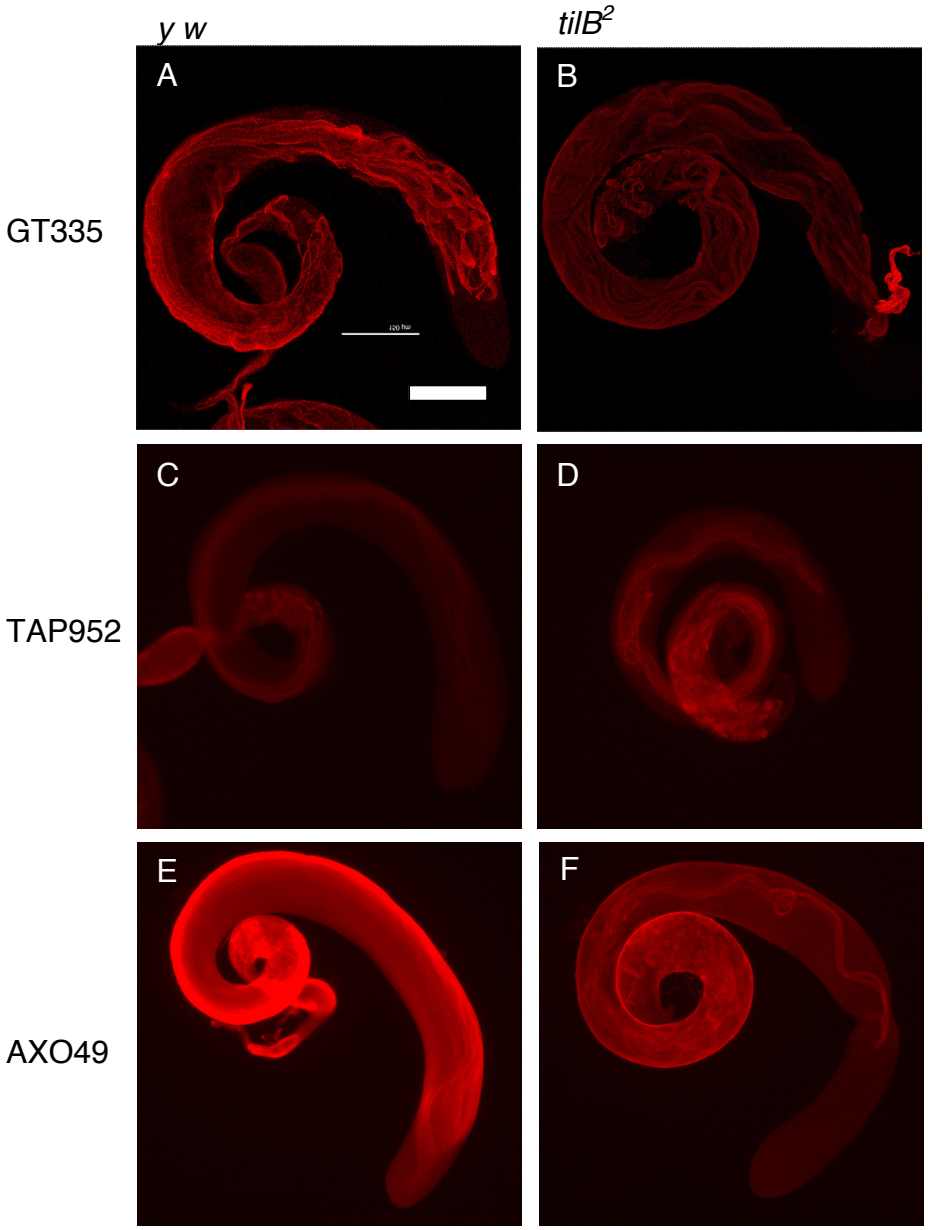

FIGURE S2.—TilB is not involved in tubulin polyglutamylation or polyglycylation.Testes from *y w* control (A,C,E) and from *tilB*^{2} mutant (B,D,F) males, stained with the GT335 antibody (A,B) to show polyglutamlylation of axonemal tubulin, and with the AXO49 and TAP952 to show tubulin polyglycylation. Both modifications are apparent in *tilB* mutant and control testes. Scale bar in A) is 200μm for all panels.

TABLE S1

Primers used to characterize *tilB*

	Forward Primer	Reverse primer
Sequencing	CAACGTCCACAAACCAATCC	GAACAATGATGGACCGGTTC
CG14620		
	GGTCACCTTGTGGTCAATCT	CATTATCCGACTTACGTTAC
	GAGAGCTAACCAGTGTTGAG	CTTACCTGTACACCTCCAGT
	AGATTCGCACAGAGATCGCT	TGCTGATGTCCACTACTCCT
Sequencing	GTCCGGTTATCGATATCTGA	GGATACGATCGGTAATGCGA
CG14617		
	ACCATACAGGTGGATCCTCC	GGTTAAGCTGCTGTTCCGGA
	CGGAACAGCAGCTTAACCAA	TGACTACCCGAATTGCTAGG
	GTAGTCAGTTATGCAAGTGC	CCCATTTACTCGTAGAGTAC
	CTCAAACATCGCCGATTGGA	GAAAGCTCCGCAATGTCTTG
	GGGTAGATTCGGTAGTATCC	TCCAACTCGGTGTAGGACAT
Genomic Rescue	CGTTCTGAAAGATCCAGGCA	AGTAGCCGGCAACAACGCTT
tilB RT-PCR	AGATTCGCACAGAGATCGCT	TGCTGATGTCCACTACTCCT
VLRR and VLRRCC	CAACTTCAAGATCCGCCAA	AATGAGTACCAACTCGCGGA